sustainability

MDPI

Article

Seasonal Dynamics and Source Apportionment of Heavy Metals in Road Dust: A Case Study of Liuzhou, China

Lu Zhang, Jianping Qian *, Jinrui Liu, Kangkang Niu and Huanrong Zhang

College of Earth Sciences, Guilin University of Technology, Guilin 541004, China
* Correspondence: q146219@163.com

Abstract: The spatial distribution and seasonal variation in heavy metal pollution in road dust in Liuzhou, China, were investigated. Road dust samples were collected during both drought and wet periods, and the concentrations of nine heavy metals—Cr, Ni, Cu, Pb, Zn, Cd, As, Sb, and Hg—were analyzed. The analysis showed that all nine heavy metals were higher than the background values of Chinese urban soils in both the drought and wet periods, and the mean heavy metal contents of road dust in the dry period were higher than those in the wet period, except for Cd. In the assessment of the pollution of heavy metals in road dust, the results of Igeo showed that Cd and Hg were significant; the results of NI showed that Cr and Ni were more significant. The spatial analysis shows that the industrial concentration areas in the north and west of Liuzhou City are concentration areas of heavy metal pollution. A Pearson correlation analysis showed high correlation between Cd in road dust heavy metals and Cd in the surrounding soil. Source identification via PCA revealed four main contributors: metallurgical and coal-fired industries, mechanical manufacturing, green belt maintenance, and waste treatment facilities. A quantitative analysis via APCS-MLR modeling confirmed that metallurgical and coal-fired industrial sources are the most widespread and important pollution sources in Liuzhou. There is a significant increase in the contribution of waste treatment sources to Hg contamination during wet periods.

Keywords: road dust; soil; heavy metals pollution; seasonal dynamics; source apportionment

Citation: Zhang, L.; Qian, J.; Liu, J.; Niu, K.; Zhang, H. Seasonal Dynamics and Source Apportionment of Heavy Metals in Road Dust: A Case Study of Liuzhou, China. *Sustainability* **2024**, *16*, 10051. https://doi.org/10.3390/su162210051

Academic Editor: Teodor Rusu

Received: 2 November 2024
Revised: 10 November 2024
Accepted: 15 November 2024
Published: 18 November 2024

1. Introduction

In recent decades, with the acceleration in industrialization and the continuous expansion of urbanization in China, the development of industrial cities has become a key driver of national economic growth [1]. However, this rapid development has also resulted in numerous environmental issues, with heavy metal pollution in road dust of particular concern [2,3]. Road dust, which is a distinct urban environmental component, functions as both a sink and a source of pollutants [4] and serves as a vital connection between the atmosphere, soil, and water [5,6]. Road dust refers to fine particulate matter suspended in air as a result of various factors, including human activities, transportation, and construction in urban environments [7,8]. These particles include but are not limited to soil particles, construction material debris, vehicle exhaust particles, industrial emissions, plant pollen, and atmospheric aerosols, with sizes ranging from a few micrometers to several tens of micrometers [9–11]. Heavy metals in these particles can enter the human body via inhalation, ingestion, and skin contact, where they can accumulate in various organs and tissues [12,13]. This accumulation can cause severe damage to the nervous, hematopoietic, renal, and reproductive systems, leading to acute or chronic diseases, including cancer, and even death, thus posing a serious threat to human health [14,15].

Heavy metal pollution in road dust is influenced by various sources, including industrial, residential, traffic-related, and natural sources, with industrial pollution as the most significant contributor [16]. In cities where heavy industry plays a dominant role in the economy, emissions resulting from industrial activities profoundly impact heavy

metal pollution in road dust [17]. Major sources include emissions originating from metal smelting plants, forging mills, and steel mills, as well as smoke resulting from coal and oil combustion [18,19]. For example, in metallurgical, metal pickling, and electroplating processes, Cu, as a primary component of fossil fuels and lubricants, can be released into road dust [20]; industrial fumes generated during metallurgical and refining processes can lead to Cd, Cu, and Zn pollution [21]; and Sb, which is widely applied in metal alloys and solders, may be enriched in road dust due to its extensive use in the electronics and machinery industries [22]. Additionally, emissions originating from the electronics, paper, and pharmaceutical industries and fuel combustion contribute to the accumulation of As, Cr, Fe, and Hg in urban environments [4].

Urban transportation emissions are also a significant source of pollution. In the 20th century, the use of leaded gasoline resulted in severe Pb contamination in soils and surface dust in cities [23]. With the ban on leaded gasoline [24], the contribution of exhaust emissions to urban heavy metal pollution has markedly decreased, and noncombustion emissions have become an important source of Pb and other heavy metals [25]. Traffic-related noncombustion heavy metal pollution is concentrated in areas with high traffic density levels and is closely related to traffic flow, braking behavior, and proximity to intersections [26,27]. The primary sources include brake wear, corrosion and wear of vehicle components, leakage of lubricating oil, wear of road markings, and road surface abrasion [28]. In 2022, the number of Motor Vehicles in Liuzhou City was 1,330,500, of which the number of automobiles has exceeded 1,000,000; compared with 2012, the number of automobiles in Liuzhou City has increased by 786,000 during the 10-year period, an increase of 3.68 times (www.liuzhou.gov.cn). Urban soil is another important source of heavy metal pollution in road dust [29]. Owing to the bioaccumulative and persistent nature of heavy metals, they can enter urban soils via various pathways and remain for extended periods [30]. Anthropogenic activities such as industrial emissions, traffic pollution, construction, and waste management contribute to the accumulation of heavy metals in soil [31]. Heavy metals in soil can be resuspended in air due to wind erosion or vehicle movement, contributing to pollution in road dust [32]. Additionally, rainfall can lead to the runoff of heavy metals from soil into road dust [13,33]. Pesticides, fertilizers, and other chemicals encountered in urban soils, particularly in green spaces and areas with frequent agricultural activities, often contain heavy metals such as Cd and Pb, rendering these areas key sources of road dust pollution [34].

Liuzhou, which is a significant industrial city in China, is renowned for its long industrial history and abundant resources (www.liuzhou.gov.cn). One major initiative was the Liuzhou Environment Management Project (www.worldbank.org), which was supported by the World Bank from 2005 to 2011 and focused on increasing wastewater treatment, pollution control, and solid waste management. Despite the increasing focus on heavy metal pollution in urban environments [35,36], there remains a notable gap in understanding the seasonal variability in heavy metal concentrations and their sources in industrial cities such as Liuzhou [37]. Existing studies have focused primarily on static measurements without accounting for the fluctuations due to seasonal changes, which can significantly influence pollution patterns [38]. Additionally, while many studies have revealed general pollution sources, the application of advanced statistical models to precisely quantify such sources remains limited [39,40].

This study aimed to bridge these gaps by investigating the spatial and temporal variations in heavy metal pollution in road dust across different seasons, thereby utilizing advanced statistical techniques such as principal component analysis (PCA) and APCS-MLR modeling to identify and quantify the contributions of various pollution sources. By comprehensively applying numerical statistical analysis, pollution evaluation, spatial distribution determination, correlation analysis, PCA, and APCS-MLR modeling, this research aimed to determine the following: (1) the spatial and temporal variations and pollution levels of heavy metals in road dust; (2) the sources of heavy metal pollution in road dust; and (3) the seasonal changes in the contribution rates of pollution sources.

2. Materials and Methods

2.1. Study Area

Liuzhou city is located in the northern–central part of the Guangxi Zhuang Autonomous Region and serves as an important transportation hub connecting South China, Central China, and Southwest China. It is situated at the intersection of the Xiang-Gui, Qian-Gui, and Zhi-Liu railways, with geographic coordinates ranging from 108°32′ to 110°28′ E longitude and 23°54′ to 26°03′ N latitude. Liuzhou exhibits a subtropical monsoon climate characterized by warm and humid conditions. Rainfall is concentrated between April and August each year, accounting for approximately 70% of the total annual precipitation. The average annual rainfall ranges from 1500 to 1600 mm, with the extreme annual rainfall reaching up to 2026.5 mm (www.liuzhou.gov.cn). The seasonal distribution of rainfall significantly influences the dispersion and accumulation of heavy metal pollution in road dust in Liuzhou city [41,42].

2.2. Sample Collection

In this study, the sample size was chosen to align with the practical constraints of the study area and the available resources for sample collection and analysis. The systematic sampling method [43] employed across 160 grids of 1.5 km × 1.5 km in Liuzhou ensured comprehensive coverage of the urban area. This approach allows for a detailed examination of the spatial distribution of pollutants and provides a robust dataset for the subsequent statistical analysis. Samples (Figure 1), including road dust and soil samples, were collected during the drought period (November 2022) and the wet period (May 2023). Road dust was collected after seven consecutive days without rain, with approximately 5 g of dust collected at each site. Soil samples were collected within 30 m of the dust sampling sites in green belts at a sampling depth of 1020 cm, with approximately 1 kg of soil collected at each site. All the samples were stored in refrigerated containers and promptly transported to the laboratory for further analysis to ensure their freshness and reliability.

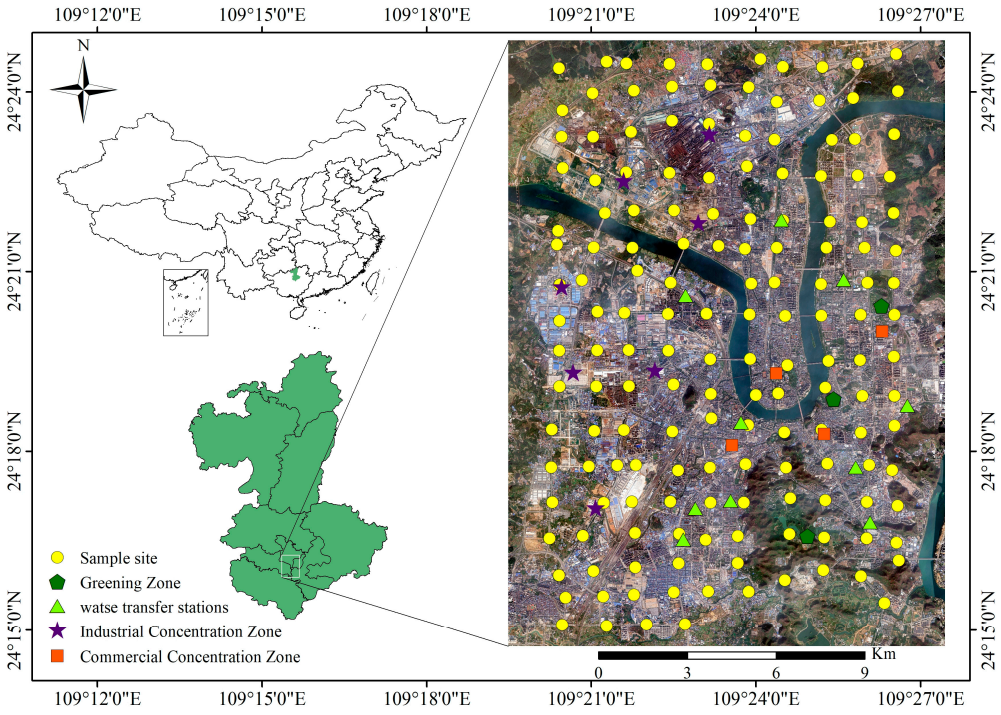

Figure 1. Location of the study area and distribution of the sample sites.

2.3. Chemical Analysis

The methods used to preprocess the road dust and soil samples included natural air drying, debris removal, grinding, and sieving. All the samples were subjected to acid

digestion via a graphite digestion instrument. The final volume was adjusted to 50 mL, and the samples were stored for analysis. Heavy metals were measured via atomic absorption spectrometry (ICP-AAS) for Cr, Ni, Cu, Pb, Zn, and Cd; via atomic fluorescence spectrometry (ICP-AFS) for As and Sb; and via an RA-915M LUMEX mercury analyzer (LUMEX instruments, Mission, BC, Canada) for Hg. During the measurements, the operational conditions (e.g., wavelength and flame temperature) were strictly controlled. Standard samples were used for calibration before each measurement, with parallel measurements conducted to ensure data accuracy. For quality control, national standard soil samples (GSS-8) were employed, and blank and parallel samples were inserted to monitor the experimental errors. The recovery rates for all the measured elements were above 85%, and the relative standard errors were smaller than 5%.

2.4. Road Dust Pollution Assessment

2.4.1. Geological Accumulation Index Method

The geological accumulation index (I_{geo}) method, first proposed by Muller [44], is a commonly employed metric for assessing the degree of heavy metal pollution in road dust. This method can be used to quantify the accumulation level and degree of heavy metal pollution via the calculation of the logarithmic ratio between the concentration of heavy metals in road dust and the geochemical background value [45]. I_{geo} can be calculated as follows [46]:

$$I_{geo} = \log_2\left(\frac{C_n}{K \times B_n}\right) \quad (1)$$

where C_n denotes the measured concentration of heavy metals in the soil or road dust samples, B_n denotes the geochemical background value of the heavy metal, and K denotes the correction factor for the geochemical background matrix. In this study, national urban soil background values were selected as background values for I_{geo} calculation [47]. Moreover, the K value was set to 1.5, which is commonly considered in such evaluations in China [34]. On the basis of the calculation results, the pollution level determined via I_{geo} can be divided into four categories: nonpollution, light pollution, moderate pollution, and heavy pollution.

2.4.2. Nemerow Pollution Index Assessment

The Nemerow composite pollution index (NI) can be used to comprehensively assess the heavy metal content in road dust. This method aims to provide pollution index values for multiple heavy metal elements, accounting for both extreme and average values [48,49]. The NI can more comprehensively reflect the pollution status of road dust [50]. The Ni can be calculated as follows [51]:

$$F_i = \frac{S_i}{B_i} \quad (2)$$

$$NI = \sqrt{\frac{F_{max}^2 + F_{ave}^2}{2}} \quad (3)$$

where F_i is the pollution index of a given heavy metal element, S_i is the measured concentration of the heavy metal, and B_i is the standard value of the heavy metal concentration, with reference to the risk screening values in GB36600-2018 [52]. Moreover, F_{max} is the maximum value among the single-factor indices of all heavy metals, and F_{ave} is the average value of the single-factor indices of all heavy metals. On the basis of the NI results, the pollution level can be categorized into four categories: nonpollution, light pollution, moderate pollution, and heavy pollution.

2.5. Source Analysis of Road Dust Pollution

2.5.1. Spatial Distribution Characteristics of Road Dust

To analyze the spatial distribution characteristics of heavy metals in road dust in Liuzhou city, kriging interpolation was employed to spatially interpolate the heavy metal concentration

data collected during the drought and wet periods. Contour maps of heavy metal concentrations were generated via Surfer 15 software. Kriging interpolation is a widely used spatial interpolation method based on regionalized variable theory [53], which can be used to effectively estimate the concentrations of heavy metals at unsampled locations [54]. The created contour maps show the spatial distribution of heavy metals across the study area, helping to identify potential pollution hotspots and pollution dispersion patterns.

2.5.2. Correlation Analysis Between Road Dust and Soil

A Pearson correlation analysis was used to explore the relationships between the heavy metal concentrations in road dust and the surrounding soil. Pearson correlation analysis is a statistical method that aims to measure the linear relationship between two variables, with the correlation coefficient r ranging from -1 to 1. Values closer to 1 or -1 indicate a stronger linear relationship [55]. A correlation analysis was performed via IBM SPSS Statistics 27 software, and the results helped determine whether road dust and soil shared common pollution sources [56]. This analysis is crucial for identifying the extent to which heavy metals in the surrounding soil contribute to the levels of heavy metals measured in road dust.

2.5.3. Principal Component Analysis (PCA) to Analyze Pollution Sources

PCA was applied to analyze the relationships between the different heavy metal elements in road dust. PCA is a statistical technique that aims to reduce the dimensionality of a given dataset by transforming correlated variables into a smaller set of uncorrelated variables, referred to as principal components. This method is particularly useful for identifying potential pollution sources [57]. The principal component analysis of heavy metals in road dust is preceded by the Kaiser-Meyer-Olkin (KMO) test and Bartlett's sphericity test; the KMO sampling adequacy quantities need to be greater than the test requirement of 0.5, and the Bartlett's sphericity test significance requirement is less than 0.005 [58].

In this study, PCA was employed to analyze the data for heavy metals in road dust, with the goal of identifying the common pollution sources. The covariance or correlation matrix was calculated to determine the relationships between the heavy metal concentrations. Eigenvalues and eigenvectors were obtained, with the eigenvalues representing the variance explained by each principal component and the eigenvectors indicating the direction of each component. The principal components are linear combinations of the original heavy metal concentrations and provide insights into common pollution sources among the different heavy metals [59,60]. The principal component score can be calculated as follows:

$$Z_i = \sum_{j=1}^{n} e_{ij} x_j \quad (4)$$

where Z_i is the score of the i-th principal component, e_{ij} is an element of the eigenvector, and x_j is the observation of the original variable. By analyzing these scores, the contributions of major pollution sources to the measured heavy metal concentrations in road dust were determined.

2.5.4. APCS-MLR Model Analysis to Quantify Pollution Source Contributions

The APCS-MLR model represents the combination of PCA and multiple linear regression (MLR) and can be used to quantify the contributions of different pollution sources to the measured heavy metal concentrations in road dust [61]. First, major pollution source factors were extracted via PCA, and the absolute principal component scores (APCSs) for each sample were calculated. The APCS can be calculated as follows:

$$\mathrm{APCS} = \mathrm{Z_i} - \mathrm{Z_{0i}} \quad (5)$$

where Z_i is the principal component score of sample i and Z_{i0} is the principal component score of a zero-concentration sample. Z_{0i} can be calculated as follows:

$$Z_{i0} = \frac{0 - \overline{C}_i}{\sigma_i} = -\frac{\overline{C}_i}{\sigma_i} \quad (6)$$

Next, MLR was applied with the APCS as the independent variable and the heavy metal concentration as the dependent variable to establish a regression model for quantifying the contribution of each pollution source to the concentration of each heavy metal. The MLR regression equation can be expressed as follows:

$$C_i = b_{i0} + \sum_{P=1}^{P} (b_{Pi} \times APCS_P) \quad (7)$$

where C_i is the predicted concentration of a given heavy metal in sample i, b_{i0} is the regression constant, b_{Pi} is the regression coefficient, and $APCS_P$ is the absolute principal component score of factor P. By analyzing the regression coefficients, the contribution of each pollution source to the measured heavy metal concentrations in road dust was quantified [59,62].

3. Results and Discussion

3.1. Characterization of the Concentrations of Heavy Metal Elements in Road Dust

The results of the statistical analysis of the heavy metals (Cr, Ni, Cu, Pb, Zn, Cd, As, Sb, and Hg) in road dust and the surrounding soil in Liuzhou city are summarized in Table 1. During the drought period, the concentrations of heavy metals indicated the descending order of Zn > Pb > Cu > Cr > Ni > As > Sb > Cd > Hg. The average concentration of Zn was approximately 4.9 times greater than the national soil background value of 71.00 mg/kg, that of Pb was approximately 9.8 times greater than the background value of 28.00 mg/kg, and that of Cu was approximately 12.7 times greater than the background value of 20.00 mg/kg, indicating relatively severe pollution. In contrast, although the average Cd and Hg concentrations were relatively low, they were still 10 and 30 times higher, respectively, than the background value of 0.08 mg/kg. The coefficients of variation of Cd, Hg, and As were 205.26%, 140.25%, and 112.90%, respectively, which were all exceeding 100%, indicating that these metals exhibited a wide distribution range and possible significant pollution sources in certain areas [63].

During the wet period (Table 1), the concentrations of heavy metals followed the order of Zn > Pb > Cr > Cu > Ni > As > Sb > Cd > Hg. Although the concentrations of most heavy metals decreased during the wet period, the Pb and Zn pollution levels remained high, at 7.5 and 3.3 times the background values, respectively. The average Cd and Hg concentrations were 10.6 and 14.5 times greater, respectively, than the background values, with coefficients of variation of 27.86% and 184.34%, respectively. The high coefficients of variation of Hg and Ni (both exceeding 100%) suggest that the distributions of these heavy metals varied significantly across the different sampling sites, likely because of the environmental conditions during the wet period, which may have exacerbated the spatial heterogeneity in pollution [17,64].

In the surrounding soil (Table 1), the concentrations of heavy metals followed the order of Pb > Ni > Zn > Cu > Cr > As > Sb > Cd > Hg. The average Cd concentration was 14.5 times greater than the national soil background value, that of As was 6.35 times greater than the national soil background value, and that of Ni was 4.3 times greater than the national soil background value. The concentrations of these heavy metals in the surrounding soil were considerably higher than those in road dust during both the drought and wet periods, suggesting that the high Cd, As, and Ni levels in road dust may be influenced by the surrounding soil.

A comparison of the heavy metal contents in road dust and soil across the different periods (Table 1) revealed that seasonal climate changes significantly impacted the distribution of heavy metals in road dust. Increased rainfall during the wet period led to a general

decrease in the heavy metal content in road dust, whereas the decrease in rainfall during the drought period resulted in the accumulation of these elements in road dust, causing a significant increase in their concentrations. Despite the lower average concentrations during the wet period, Hg maintained a high coefficient of variation, indicating that Hg was influenced by specific pollution sources that were independent of seasonal environmental changes. In the surrounding soil, the contents of heavy metals such as Cd, As, and Ni were significantly greater than those in road dust, indicating that these elements may be influenced primarily by the soil itself, whereas other elements such as Cr, Cu, Zn, and Hg likely originated from additional pollution sources.

Table 1. Descriptive statistics of heavy metals in road dust and surrounding soil in Liuzhou city (mg kg^{-1}).

Sample		Cr	Ni	Cu	Pb	Zn	Cd	As	Sb	Hg
Drought period (n = 160)	Minimum	26.54	25.84	31.82	68.82	87.18	0.11	8.36	3.82	0.03
	Maximum	580.67	346.99	1879.00	814.36	1437.71	20.69	259.22	147.27	5.76
	Mean	129.16	58.05	254.40	274.69	346.63	0.80	31.80	23.29	0.60
	Standard deviation	88.84	46.88	236.94	136.18	194.21	1.65	35.90	21.55	0.84
	Coefficient of variation (%)	68.78	80.76	93.14	49.58	56.03	205.26	112.90	92.53	140.25
Wet period (n = 160)	Minimum	9.67	1.73	6.11	0.81	7.35	0.60	0.66	0.02	0.01
	Maximum	564.34	384.55	688.88	587.61	969.84	2.81	55.62	10.30	4.48
	Mean	117.63	45.45	104.30	210.87	235.02	0.85	25.26	2.49	0.29
	Standard deviation	74.25	47.76	74.52	109.94	147.31	0.24	11.23	1.66	0.54
	Coefficient of variation (%)	63.12	105.08	71.45	52.14	62.68	27.86	44.44	66.50	184.34
Surrounding soil mean (n = 160)		42.94	123.76	91.49	269.15	120.40	1.16	107.93	12.45	0.28
Soil background of China *		70.00	29.00	20.00	28.00	71.00	0.08	17.00	1.40	0.02

* Geochemical background and baseline values of chemical elements in urban soil in China [47].

3.2. Assessment of Heavy Metal Pollution

The I_{geo} values for the nine heavy metals in road dust during both the drought and wet periods in Liuzhou city were calculated and are shown in Figure 2a. The results revealed that the mean Igeo values for Cr, Ni, and As during both periods were close to the nonpollution threshold. The minimum Igeo values for these metals fell within the nonpolluted category, while their maximum values reached the light to moderate pollution levels. This indicates that the pollution levels of these three heavy metals were relatively low, with minimal seasonal influences. The variation in the Igeo values between the drought and wet periods was low, suggesting that the release of these metals was less affected by seasonal fluctuations. However, the mean Igeo values for Cu, Pb, Cd, Sb, and Hg (except for Cu and Sb during the wet period) reached the moderate pollution level. The maximum Igeo values for Cu, Cd, Sb, and Hg during the drought period reached the severe pollution level. Cd and Hg also exhibited high pollution levels during the wet period, indicating that these two metals may have been influenced by long-term, stable pollution sources in the study area. Significant seasonal variation in Igeo was observed for Cu, Pb, Zn, Cd, Sb, and Hg, with notable differences between the two periods. Except for Cd, the Igeo values for these heavy metals during the wet period were significantly lower than those during the drought period, suggesting that rainfall during the wet period alleviated pollution. In contrast, the mean Igeo value for Cd was greater during the wet period than during the drought period, indicating that Cd accumulates more easily under wet environmental conditions, further highlighting the unique nature of Cd pollution sources.

The NI values for the nine heavy metals in road dust during the drought and wet periods in Liuzhou city are shown in Figure 2b. The results indicated that the NI values for Cu, Zn, Cd, and Hg remained at the nonpolluted level during both periods, suggesting relatively low pollution stemming from these metals. However, the Cr, Ni, Pb, As, and Sb pollution levels were relatively high. The NI values for Cr and Sb during the drought period reached the moderate pollution level, whereas the NI values for Cr, Ni, and Pb during the wet period indicated slight pollution. A comparison of the NI values between the two periods revealed that the values for Cr, As, and Sb were significantly greater during the

drought period, demonstrating clear seasonal variation, with rainfall during the wet period causing a reduction in heavy metal concentrations. Notably, the NI value for Ni during the wet period was greater than that during the drought period, indicating a specificity in the pollution source for this metal during the wet period.

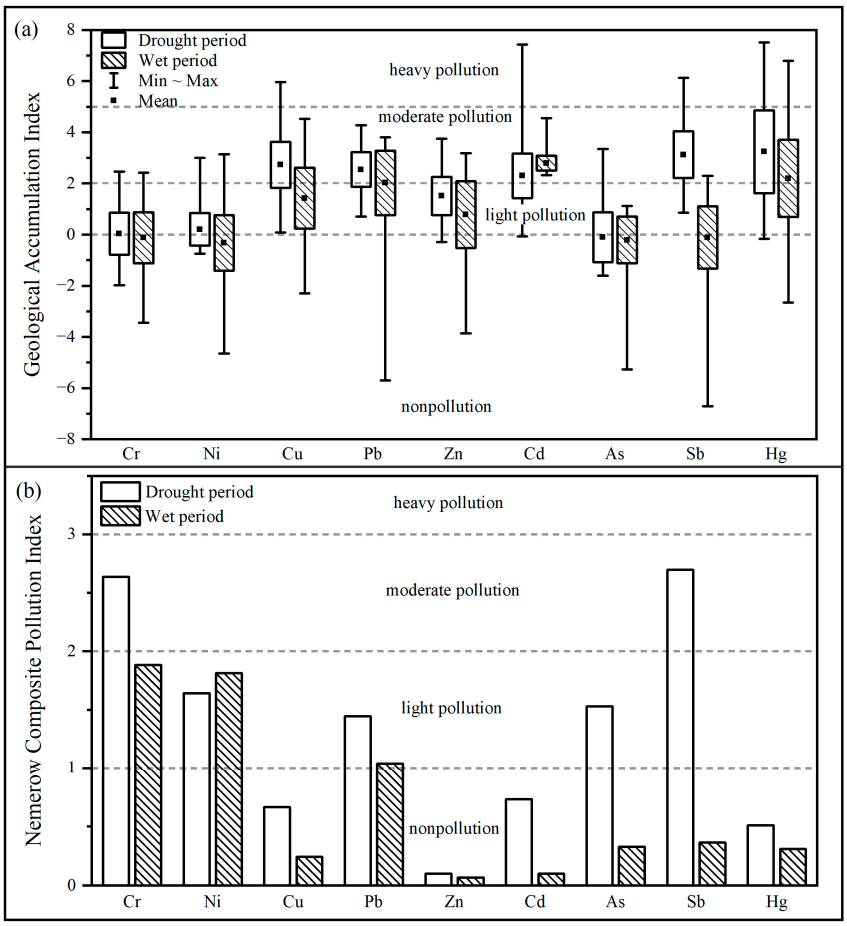

Figure 2. (**a**) Box plots of the geological accumulation index for the heavy metals in road dust. (**b**) Histogram of the Nemerow composite pollution index for the heavy metals in road dust.

3.3. Spatial Distribution of Heavy Metals in Road Dust During the Different Periods

The spatial distribution of heavy metals in road dust during the drought period revealed that Cr and Ni exhibited similar patterns (Figure 3a,b), with polluted areas primarily concentrated in the central region of Liuzhou city. This area is home to several factories, and additional polluted zones were found in the northern–central and southern–central regions, suggesting that the observed pollution could be due to migratory effects from industrial zones or contributions from other pollution sources. The spatial distributions of Cu, Pb, Zn, Cd, As, and Sb (Figure 3c–h) also demonstrated similar patterns, with polluted areas concentrated in the northern industrial zone and near major transportation routes in the western part of the city. Significant Pb, Zn, and Sb pollution hotspots (Figure 3d,e,h) occurred in the southeastern part of the city, indicating that these three metals may share common pollution sources. Hg (Figure 3i) exhibited a relatively dispersed spatial distribution, with polluted areas located in the northeastern, southwestern, and southern–central residential zones, suggesting contributions from multiple sources [11,65].

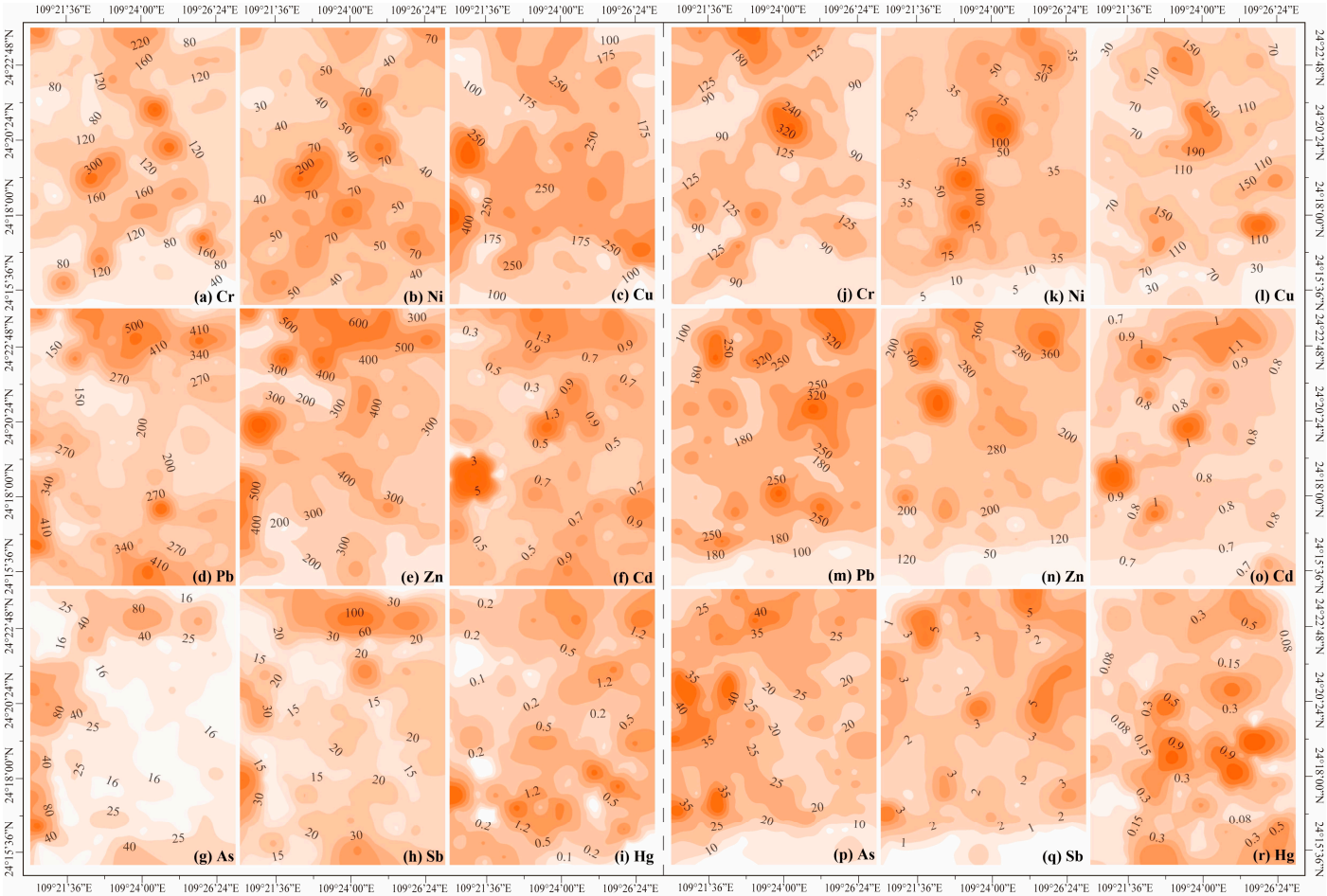

Figure 3. Spatial distribution patterns of heavy metals in road dust during the drought (**a**–**i**) and wet periods (**j**–**r**).

During the wet period, the spatial distribution of heavy metals in road dust revealed that Cr and Ni (Figure 3j,k) still exhibited similar patterns, with pollution concentrated in the northern and central areas of Liuzhou city, which is consistent with the distribution during the drought period. This indicates that the pollution sources for these two heavy metals likely occurred in the central industrial zone. High levels of Cu, Pb, Zn, Cd, As, and Sb pollution (Figure 3i–q) were observed in the northern part of the study area. When combined with the drought period data, these findings suggest that the northern industrial zone may be a consistent pollution source for these metals. Additionally, notable Cu, Pb, Zn, and Sb pollution hotspots (Figure 3l,m,n,q) were observed in residential areas, suggesting a potential pollution source within these zones. High concentrations of Hg (Figure 3r) were primarily found in the central region of the city, which is also a residential area, indicating that residential activities could contribute to Hg pollution.

These spatial distribution patterns provide insights into the characteristics of heavy metal pollution across the different areas [66]. A detailed analysis of activities in the northern industrial zone, western transportation routes, and residential zones could help to identify specific pollution sources. Field investigations in these areas revealed that the northern industrial zone includes an iron and steel plant, a steel processing plant, and a power plant. The western road is a major transportation route for factories in the northern industrial area, and the distribution of Cu, Pb, Zn, As, and Sb pollution overlaps with the geographic location of the northern industrial area and the western transportation route. In the western region, large vehicle manufacturing plants and heavy machinery production facilities, along with several smaller processing factories, overlap with the distribution of Cr and Ni pollution. In residential areas, the distribution of waste transfer stations was

identified as highly overlapping with the distribution of Hg pollution. The overlapping of heavy metal pollution distribution with anthropogenic activities can give a preliminary indication of the source of heavy metal pollution.

3.4. Correlation Analysis of Heavy Metals Between Road Dust and Surrounding Soil

During the drought period (Figure 4), Cr in road dust was strongly correlated with Cu, Pb, Zn, Sb, and Hg in the surrounding soil, with p values less than 0.001. Ni was also significantly correlated with Pb, Zn, Sb, and Hg in the surrounding soil. Pb in road dust was highly correlated with As in the surrounding soil, and Cd was highly correlated with Cd in the surrounding soil. In terms of the other heavy metals, the correlations were relatively low. During the wet period (Figure 4), Cr in road dust was strongly correlated with Zn in the surrounding soil, and Ni was strongly correlated with Zn. Pb in road dust was highly correlated with Pb, Zn, and Sb in the surrounding soil, whereas Cd was correlated with Cd in the surrounding soil. Sb was also correlated with Sb in the surrounding soil. Notably, Cu, As, and Hg in road dust were not significantly correlated with any heavy metals in the surrounding soil during either period, suggesting that the sources of these metals differed from those affecting the metals observed in the surrounding soil [67]. In contrast, Cd in road dust was consistently correlated with Cd in the surrounding soil during both periods, indicating that Cd pollution in road dust and the surrounding soil likely originated from the same source. Moreover, the significant correlations between Pb and Sb in road dust and the surrounding soil during the wet period suggested that seasonal environmental changes may cause these metal pollution sources to conform more closely with those in the surrounding soil [5,68].

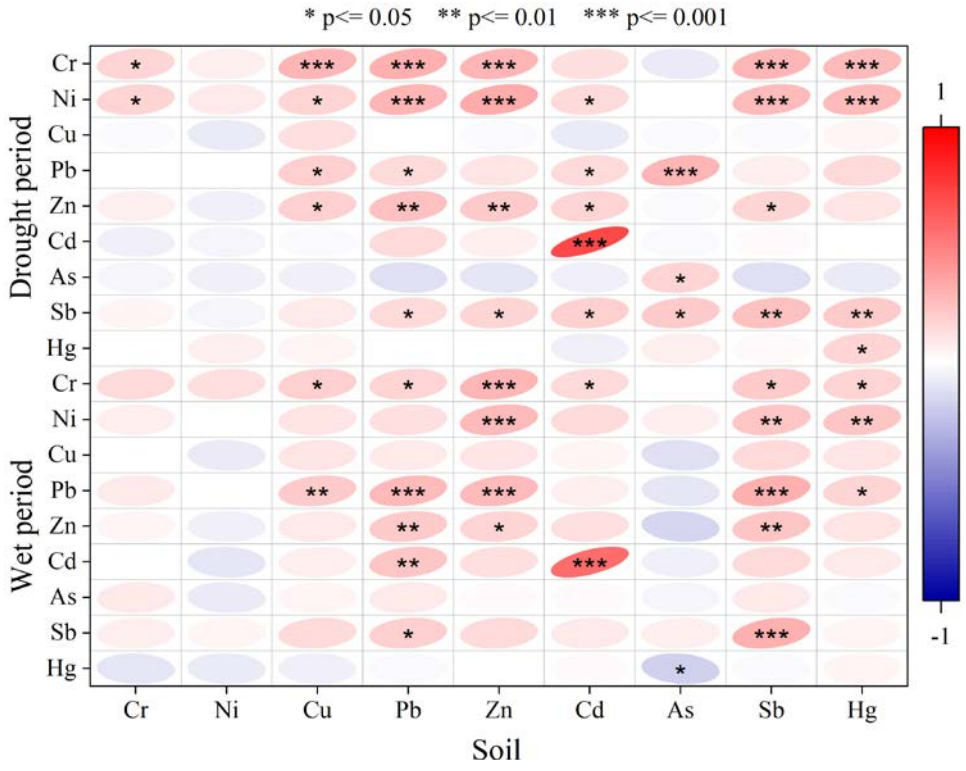

Figure 4. Thermogram of the correlations between heavy metals in the surrounding soil and road dust during the drought and wet periods.

3.5. Principal Component Analysis to Determine Pollution Sources

The KMO test results for the drought and wet periods were 0.66 and 0.79, respectively. Since both values exceeded the required threshold value of 0.5 and since Bartlett's test

values were less than 0.005, PCA was considered appropriate for analyzing the heavy metal data for both periods.

Owing to the complexity and diversity of pollution sources, PCA was used to extract several principal components that could explain the majority of the variance in the heavy metal pollution data. Four principal components were identified, which explained 75.70% and 74.02% of the total variance in pollution in road dust during the drought and wet periods (Table 2), respectively. Each principal component represents a distinct pollution source, allowing us to identify the main contributors to the measured heavy metal concentrations in road dust [69,70].

Table 2. Total variance explained and component matrices for the heavy metals during the different periods.

Variables	Drought Period				Wet Period			
	PC1	PC2	PC3	PC4	PC1	PC2	PC3	PC4
Cr	0.43	0.85	0.05	0.01	0.57	0.60	−0.30	0.04
Ni	0.24	0.90	0.07	0.03	0.52	0.62	−0.22	0.09
Cu	0.63	0.06	−0.25	−0.36	0.64	0.39	0.06	−0.01
Pb	0.75	−0.21	0.22	0.17	0.81	−0.18	0.18	−0.22
Zn	0.80	−0.07	0.11	−0.18	0.79	−0.25	0.06	−0.14
Cd	0.11	−0.12	0.92	0.12	0.47	−0.28	0.07	0.83
As	0.64	−0.39	−0.16	−0.12	0.57	−0.40	−0.31	−0.17
Sb	0.78	−0.18	−0.07	0.06	0.71	−0.35	0.15	−0.08
Hg	0.30	−0.01	−0.28	0.87	0.10	0.33	0.86	−0.02
Total	2.97	1.80	1.07	0.97	3.34	1.46	1.05	0.81
Eigenvalue of variance (%)	32.96	19.99	11.93	10.81	37.16	16.22	11.70	8.94
Total variance explained (%)	32.96	52.96	64.89	75.70	37.16	53.38	65.08	74.02

During the drought period, the PC1 component accounted for 32.96% of the total variance in the heavy metal pollution level. In PC1 during the drought period, all the heavy metal loading scores (Table 2) were greater than 0, and the loadings showed consistent trends (Figure 5a), indicating that the PC1 component contributed to all the heavy metals. Notably, the loadings for Cu, Pb, Zn, As, and Sb were 0.63, 0.75, 0.80, 0.64, and 0.78 (Table 2), respectively, indicating relatively high loadings (>0.60). The analysis of the spatial distribution characteristics of heavy metals in road dust during the drought period revealed that Cu, Pb, Zn, As, and Sb pollution (Figure 3c,d,e,g,h) was concentrated in the northern part of the study area, near steel plants and coal-fired power plants. Therefore, on the basis of the above analysis, the PC1 component during the drought period represents metallurgical and coal-fired industrial pollution sources.

The PC2 component could explain 19.99% of the total variance in the heavy metal pollution level during the drought period, in which the loading scores for Cr and Ni were 0.85 and 0.90 (Table 2), respectively, while the loading score for Cu was 0.06. The remaining heavy metals exhibited loading scores less than 0. Figure 5 shows that only Cr and Ni exhibited the same loading trend, which suggested that the PC2 component contributed to Cr and Ni pollution only during the drought period. The spatial distribution characteristics of heavy metals in road dust during the drought period revealed that Cr and Ni pollution (Figure 3a,b) was concentrated near automobile manufacturing plants and heavy machinery manufacturing plants. Therefore, on the basis of the above analysis, during the drought period, the PC2 component represents mechanical manufacturing and metal processing pollution sources.

The PC3 component during the drought period accounted for 11.93% of the total variance in the heavy metal pollution level. The loading scores for Cd, Pb, and Zn in the PC3 component were 0.92, 0.22, and 0.11, respectively, whereas the loading scores (Table 2) for the other heavy metals were less than 0.1. The consistent loading trends (Figure 5b) for Cd, Pb, and Zn indicate that the PC3 component primarily contributed to pollution of these heavy metals, with the highest contribution to Cd pollution. The spatial distribution

characteristics of heavy metals in road dust during the drought period revealed that Cd pollution (Figure 3f) was relatively dispersed. The coefficient of variation of Cd in road dust during the drought period reached 205.26% (Table 1), indicating significant anthropogenic influence. The Cd content in the surrounding soil was much higher than that in road dust and the soil background value (Table 1). Additionally, a correlation analysis revealed a highly significant correlation between Cd in road dust and Cd in the surrounding soil during the drought period (Figure 4), suggesting that Cd pollution in road dust during the drought period may have originated from the surrounding soil in green belts. The use of pesticides and growth agents during the planting and maintenance of green belts could lead to Cd enrichment in the soil, which, under the influence of weathering and rain, could migrate into road dust [71,72]. Therefore, the PC3 component represents green belt maintenance-related pollution sources.

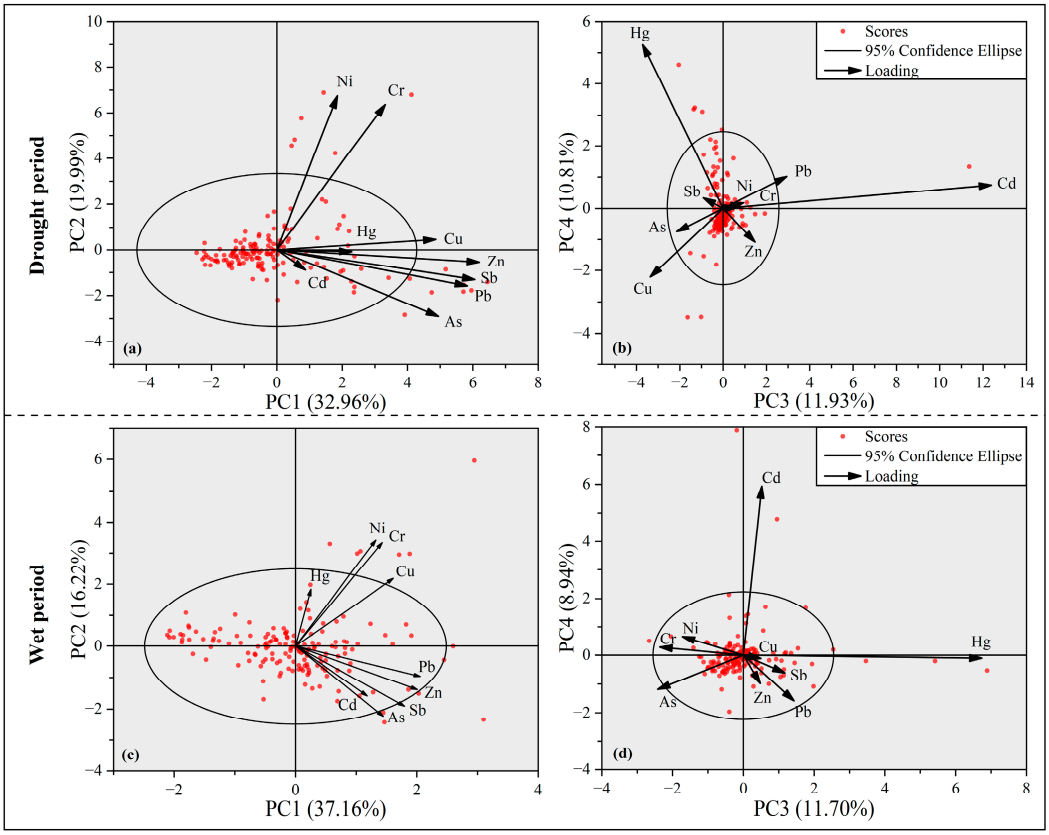

Figure 5. Graph of the principal component analysis loading trends during the different periods. Principal components (PC1, 2, 3, and 4).

The PC4 component during the drought period accounted for 10.81% of the total variance in the heavy metal pollution level. The loading score for Hg in the PC4 component was 0.87, whereas the loading scores for Pb and Cd were 0.17 and 0.12 (Table 2), respectively, with the loading scores for the other heavy metals lower than 0.1. The loading trends for Hg, Pb, and Cd in the PC4 component (Figure 5b) suggested that this principal component contributed the most to Hg pollution, with lower contributions to Pb and Cd pollution. The spatial distribution characteristics of heavy metals in road dust during the drought period revealed that Hg pollution (Figure 3i) was concentrated near residential areas and coincided with the locations of waste transfer stations. On the basis of these observations [73,74], the PC4 component during the drought period represents waste treatment pollution sources.

During the wet period, the PC1 component accounted for 37.16% of the total variance in the heavy metal pollution level. The loading scores and trends of heavy metals in the PC1

component during the wet period were consistent with those during the drought period (Table 2 and Figure 5c). However, during the wet period, PC1 also exhibited increased contributions to Cr, Ni, and Cd pollution. The spatial distribution characteristics of heavy metals in road dust during the wet period (Figure 3l,m,n,p,q) further revealed that Cu, Pb, Zn, As, and Sb pollution was concentrated near steel plants and coal-fired power plants. Therefore, PC1 represents metallurgical and coal-fired industrial pollution sources during the wet period.

The PC2 component during the wet period accounted for 16.22% of the total variance in the heavy metal pollution level, with loading scores (Table 2) of 0.60, 0.62, 0.39, and 0.33 for Cr, Ni, Cu, and Hg, respectively, as well as consistent loading trends (Figure 5c) for these heavy metals. Among these, Cr and Ni exhibited the highest loading scores and the most significant trends in the PC2 component. The spatial distribution characteristics of the heavy metals revealed that Cr and Ni pollution (Figure 3j,k) was concentrated near automobile manufacturing plants and heavy machinery manufacturing plants. Therefore, on the basis of the above analysis, PC2 during the wet period also represents mechanical manufacturing and metal processing pollution sources.

The PC3 component during the wet period accounted for 11.70% of the total variance in the heavy metal pollution level, with loading scores (Table 2) of 0.86, 0.18, and 0.15 for Hg, Pb, and Sb, respectively. The loading trend for Hg in the PC3 component during the wet period (Figure 5d) was most significant, and the spatial distribution characteristics revealed that Hg pollution (Figure 3r) was concentrated around waste transfer stations. Therefore, on the basis of the above analysis, PC3 during the wet period represents waste treatment pollution sources.

The PC4 component during the wet period accounted for 8.94% of the total variance in the heavy metal pollution level, with a loading score of 0.83 for Cd, whereas the loading scores for the other heavy metals were less than 0.1 (Table 2). The loading trend for Cd in the PC4 component during the wet period (Figure 5d) was most specific. The correlation analysis results (Figure 4) revealed a highly significant correlation between Cd in the surrounding soil and Cd in road dust during the wet period, and the Cd content in the surrounding soil was much greater than that in road dust during the wet period (Table 1). On the basis of the above analysis, pollution encompassed initial enrichment in the soil and subsequent migration into road dust. Therefore, PC4 during the wet period represents green belt maintenance-related pollution sources.

3.6. APCS-MLR Modeling for Quantitative Analysis of Pollution Sources

The APCS-MLR model was employed to quantify the contributions of the various pollution sources to the heavy metal concentrations in road dust during the drought and wet periods. The results are shown in Figure 6, which shows the quantitative contribution rates of the four major pollution sources—metallurgical and coal-fired industrial sources, mechanical manufacturing and metal processing sources, green belt maintenance sources, and waste treatment sources—to Cr, Ni, Cu, Pb, Zn, Cd, As, Sb, and Hg.

During the drought period, metallurgical and coal-fired industrial sources contributed 66% to the total Cu concentration, 67% to the total Pb concentration, 79% to the total Zn concentration, 77% to the total As concentration, and 75% to the total Sb concentration, rendering them the primary sources of these metals. Notably, mechanical manufacturing and metal processing sources were responsible for 78% of the observed Cr pollution and 89% of the observed Ni pollution, establishing them as the dominant sources for these two metals. Green belt maintenance sources contributed 69% to the total Cd pollution level, whereas waste treatment sources were the primary contributors to the total Hg pollution level, with a contribution rate of 59%. During the wet period, the contribution of metallurgical and coal-fired industrial sources increased for Ni, Pb, Zn, and Cd, with rates of 16% for Cr, 76% for Pb, 84% for Zn, and 39% for Cd. Mechanical manufacturing and metal processing sources remained the primary contributors to Cr and Ni pollution, with contribution rates of 76% and 77%, respectively. Green belt maintenance sources

contributed 60% to the total Cd pollution level, similar to that during the drought period, whereas waste treatment sources contributed 74% to the total Hg pollution level, an increase from that during the drought period.

A comparison of the pollution contribution ratios of the four sources to heavy metals in road dust during the two periods clearly revealed that the contributions of metallurgical and coal-fired industrial sources to Ni, Pb, Zn, and Cd increased during the wet period compared with those during the drought period, whereas the contributions to Cr, Cu, As, Sb, and Hg pollution decreased. The reduction in the contributions to these metals during the wet period may be attributed to the washing effect of rainwater and changes in temperature [75,76], which reduced their accumulation in road dust. However, more attention should be given to metals whose contributions increase with seasonal changes, and targeted prevention and control measures should be implemented to address these anomalies. For mechanical manufacturing and metal processing sources, the contributions to Cr, Ni, and As pollution decreased during the wet period, indicating that seasonal changes imposed a diluting effect on these metals [77,78]. However, the contribution to Cu increased from 18% to 35%. With respect to green belt maintenance sources, the contributions to Pb, Cd, and Sb decreased during the wet period, suggesting that fewer of these metals were released due to seasonal effects. However, the contribution of waste treatment sources to Hg pollution increased from 59% during the drought period to 74% during the wet period, likely due to the increased rainfall levels and lower temperatures, which facilitated Hg release from these sources.

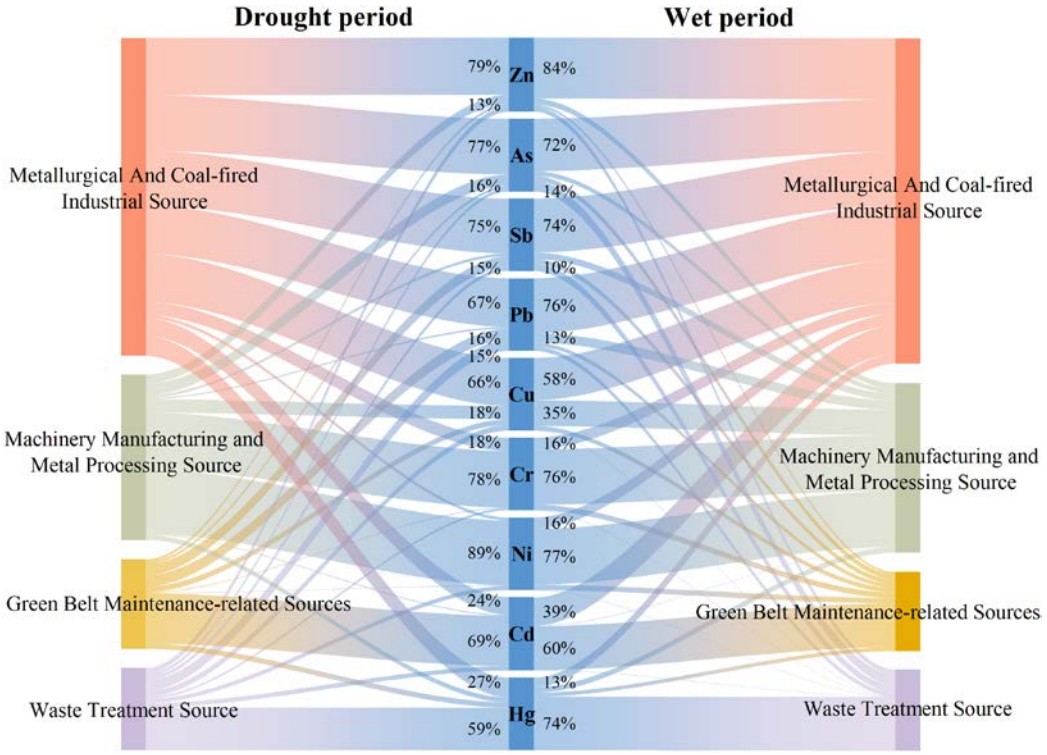

Figure 6. Sankey diagram of the quantitative contributions of the various heavy metal pollution sources.

These findings indicated that metallurgical and coal-fired industrial sources are the most widespread and important pollution sources in Liuzhou, followed by mechanical manufacturing and metal processing sources. Green belt maintenance and waste treatment sources, while less significant overall, were the primary contributors to Cd and Hg pollution levels, respectively. The seasonal variations in pollution contributions highlight the need for targeted pollution control measures that account for both industrial and environmental factors.

4. Conclusions

This study provides an in-depth analysis of the seasonal variations and source contributions to heavy metal pollution in road dust in Liuzhou city. The findings highlighted the influence of both industrial activities and environmental factors on pollution patterns. Metallurgical and coal-fired industries were identified as the primary sources of Cu, Pb, Zn, and As pollution, with their contributions to Ni, Pb, Zn, and Cd pollution increasing during the wet period due to rainfall effects. Conversely, the contributions to Cr, Cu, As, Sb, and Hg pollution from these sources decreased during the same period, likely due to the washing effect of rain. Mechanical manufacturing and metal processing were significant contributors to Cr and Ni pollution, with an increase in Cu pollution during the wet period. The influence of green belt maintenance on Cd pollution was greatest, which decreased slightly during the wet period. Waste treatment sources, particularly for Hg, demonstrated a notable increase in contribution during the wet period, reflecting seasonal environmental changes. Overall, this study demonstrates the need for targeted pollution control measures that account for seasonal changes, especially in industrial cities such as Liuzhou. By applying advanced statistical models, this research provides a comprehensive understanding of the variability in pollution sources and their contributions, offering valuable insights for environmental management and public health protection.

Author Contributions: L.Z.: writing—original draft, editing, formal analysis. J.Q.: supervision, software, review, funding acquisition. J.L.: resources, formal analysis. K.N.: draft, methodology, conceptualization. H.Z.: validation, data curation. All authors have read and agreed to the published version of the manuscript.

Funding: This work was financially supported by the National Natural Science Foundation of China (Grant No. 41561095).

Institutional Review Board Statement: Not applicable.

Informed Consent Statement: Not applicable.

Data Availability Statement: The data presented in this study are available from the corresponding author on request.

Conflicts of Interest: The authors declare no conflicts of interest. The funders had no role in the design of the study; in the collection, analyses, or interpretation of data; in the writing of the manuscript; or in the decision to publish the results.

References

1. Liu, J.; Wang, R.S.; Tian, Y.; Zhang, M.R. The driving mechanisms of industrial air pollution spatial correlation networks: A case study of 168 Chinese cities. *J. Clean. Prod.* **2024**, *470*, 143255. [CrossRef]
2. Proshad, R.; Kormoker, T.; Al, M.A.; Islam, M.S.; Khadka, S.; Idris, A.M. Receptor model-based source apportionment and ecological risk of metals in sediments of an urban river in Bangladesh. *J. Hazard. Mater.* **2022**, *423*, 127030. [CrossRef] [PubMed]
3. Lu, X.W.; Wang, Z.Z.; Chen, Y.R.; Yang, Y.F.; Fan, X.Y.; Wang, L.Q.; Yu, B.; Lei, K.; Zuo, L.; Fan, P.; et al. Source-specific probabilistic risk evaluation of potentially toxic metal(loid) s in fine dust of college campuses based on positive matrix factorization and Monte Carlo simulation. *J. Environ. Manag.* **2023**, *347*, 119056. [CrossRef] [PubMed]
4. Men, C.; Liu, R.M.; Xu, F.; Wang, Q.R.; Guo, L.J.; Shen, Z.Y. Pollution characteristics, risk assessment, and source apportionment of heavy metals in road dust in Beijing, China. *Sci. Total Environ.* **2018**, *612*, 138–147. [CrossRef]
5. Kolakkandi, V.; Sharma, B.; Rana, A.; Dey, S.; Rawat, P.; Sarkar, S. Spatially resolved distribution, sources and health risks of heavy metals in size-fractionated road dust from 57 sites across megacity Kolkata, India. *Sci. Total Environ.* **2020**, *705*, 135805. [CrossRef]
6. Yang, Y.F.; Lu, X.W.; Fan, P.; Yu, B.; Wang, L.Q.; Lei, K.; Zuo, L. Multi-element features and trace metal sources of road sediment from a mega heavy industrial city in North China. *Chemosphere* **2023**, *311*, 137093. [CrossRef]
7. Han, Q.; Wang, M.S.; Cao, J.L.; Gui, C.L.; Liu, Y.P.; He, X.D.; He, Y.C.; Liu, Y. Health risk assessment and bioaccessibilities of heavy metals for children in soil and dust from urban parks and schools of Jiaozuo, China. *Ecotoxicol. Environ. Saf.* **2020**, *191*, 110157. [CrossRef]
8. Men, C.; Liu, R.M.; Xu, L.B.; Wang, Q.R.; Guo, L.J.; Miao, Y.X.; Shen, Z.Y. Source-specific ecological risk analysis and critical source identification of heavy metals in road dust in Beijing, China. *J. Hazard. Mater.* **2020**, *388*, 121763. [CrossRef]
9. Shabbaj, I.I.; Alghamdi, M.A.; Shamy, M.; Hassan, S.K.; Alsharif, M.M.; Khoder, M.I. Risk Assessment and Implication of Human Exposure to Road Dust Heavy Metals in Jeddah, Saudi Arabia. *Int. J. Environ. Res. Public Health* **2018**, *15*, 36. [CrossRef]

10. Fan, X.Y.; Lu, X.W.; Yu, B.; Zuo, L.; Fan, P.; Yang, Y.F.; Zhuang, S.K.; Liu, H.M.; Qin, Q. Risk and sources of heavy metals and metalloids in dust from university campuses: A case study of Xi'an, China. *Environ. Res.* **2021**, *202*, 111703. [CrossRef]
11. Hao, Q.; Lu, X.W.; Yu, B.; Yang, Y.F.; Lei, K.; Pan, H.Y.; Gao, Y.H.; Liu, P.R.; Wang, Z.Z. Sources and probabilistic ecological-health risks of heavy metals in road dust from urban areas in a typical industrial city. *Urban Clim.* **2023**, *52*, 101730. [CrossRef]
12. Toth, G.; Hermann, T.; Da Silva, M.R.; Montanarella, L. Heavy metals in agricultural soils of the European Union with implications for food safety. *Environ. Int.* **2016**, *88*, 299–309. [CrossRef] [PubMed]
13. Han, Q.; Liu, Y.; Feng, X.X.; Mao, P.; Sun, A.; Wang, M.Y.; Wang, M.S. Pollution effect assessment of industrial activities on potentially toxic metal distribution in windowsill dust and surface soil in central China. *Sci. Total Environ.* **2021**, *759*, 144023. [CrossRef] [PubMed]
14. Noli, F.; Tsamos, P. Concentration of heavy metals and trace elements in soils, waters and vegetables and assessment of health risk in the vicinity of a lignite-fired power plant. *Sci. Total Environ.* **2016**, *563*, 377–385. [CrossRef]
15. Yang, S.C.; Liu, J.L.; Bi, X.Y.; Ning, Y.Q.; Qiao, S.Y.; Yu, Q.Q.; Zhang, J. Risks related to heavy metal pollution in urban construction dust fall of fast-developing Chinese cities. *Ecotoxicol. Environ. Saf.* **2020**, *197*, 110628. [CrossRef]
16. Pan, H.Y.; Lu, X.W.; Lei, K. A comprehensive analysis of heavy metals in urban road dust of Xi'an, China: Contamination, source apportionment and spatial distribution. *Sci. Total Environ.* **2017**, *609*, 1361–1369. [CrossRef]
17. Lu, X.W.; Wang, L.J.; Li, L.Y.; Lei, K.; Huang, L.; Kang, D. Multivariate statistical analysis of heavy metals in street dust of Baoji, NW China. *J. Hazard. Mater.* **2010**, *173*, 744–749. [CrossRef]
18. Kong, S.F.; Lu, B.; Bai, Z.P.; Zhao, X.Y.; Chen, L.; Han, B.; Li, Z.Y.; Ji, Y.Q.; Xu, Y.H.; Liu, Y. Potential threat of heavy metals in re-suspended dusts on building surfaces in oilfield city. *Atmos. Environ.* **2011**, *45*, 4192–4204. [CrossRef]
19. Zhang, M.M.; Lu, X.W.; Chen, H.; Gao, P.P.; Fu, Y. Multi-element characterization and source identification of trace metal in road dust from an industrial city in semi-humid area of Northwest China. *J. Radioanal. Nucl. Chem.* **2015**, *303*, 637–646. [CrossRef]
20. Ali, M.U.; Liu, G.J.; Yousaf, B.; Abbas, Q.; Ullah, H.; Munir, M.A.M.; Fu, B. Pollution characteristics and human health risks of potentially (eco) toxic elements (PTEs) in road dust from metropolitan area of Hefei, China. *Chemosphere* **2017**, *181*, 111–121. [CrossRef]
21. Christoforidis, A.; Stamatis, N. Heavy metal contamination in street dust and roadside soil along the major national road in Kavala's region, Greece. *Geoderma* **2009**, *151*, 257–263. [CrossRef]
22. Li, X.P.; Zhang, M.; Gao, Y.; Zhang, Y.C.; Zhang, X.; Yan, X.Y.; Wang, S.; Yang, R.; Liu, B.; Yu, H.T. Urban street dust bound 24 potentially toxic metal/metalloids (PTMs) from Xining valley-city, NW China: Spatial occurrences, sources and health risks. *Ecotoxicol. Environ. Saf.* **2018**, *162*, 474–487. [CrossRef] [PubMed]
23. Sezgin, N.; Ozcan, H.K.; Demir, G.; Nemlioglu, S.; Bayat, C. Determination of heavy metal concentrations in street dusts in Istanbul E-5 highway. *Environ. Int.* **2004**, *29*, 979–985. [CrossRef] [PubMed]
24. Tang, Z.W.; Chai, M.; Cheng, J.L.; Jin, J.; Yang, Y.F.; Nie, Z.Q.; Huang, Q.F.; Li, Y.H. Contamination and health risks of heavy metals in street dust from a coal-mining city in eastern China. *Ecotoxicol. Environ. Saf.* **2017**, *138*, 83–91. [CrossRef]
25. Resongles, E.; Dietze, V.; Green, D.C.; Harrison, R.M.; Ochoa-Gonzalez, R.; Tremper, A.H.; Weiss, D.J. Strong evidence for the continued contribution of lead deposited during the 20th century to the atmospheric environment in London of today. *Proc. Natl. Acad. Sci. USA* **2021**, *118*, e2102791118. [CrossRef]
26. Dousova, B.; Lhotka, M.; Buzek, F.; Cejkova, B.; Jackova, I.; Bednar, V.; Hajek, P. Environmental interaction of antimony and arsenic near busy traffic nodes. *Sci. Total Environ.* **2020**, *702*, 134642. [CrossRef]
27. Gietl, J.K.; Lawrence, R.; Thorpe, A.J.; Harrison, R.M. Identification of brake wear particles and derivation of a quantitative tracer for brake dust at a major road. *Atmos. Environ.* **2010**, *44*, 141–146. [CrossRef]
28. Adachi, K.; Tainosho, Y. Characterization of heavy metal particles embedded in tire dust. *Environ. Int.* **2004**, *30*, 1009–1017. [CrossRef]
29. Wang, S.Y.; Wang, L.Q.; Huan, Y.Z.; Wang, R.; Liang, T. Concentrations, spatial distribution, sources and environmental health risks of potentially toxic elements in urban road dust across China. *Sci. Total Environ.* **2022**, *805*, 150266. [CrossRef]
30. Wang, Y.Q.; Bai, Y.R.; Wang, J.Y. Distribution of urban soil heavy metal and pollution evaluation in different functional zones of Yinchuan city. *Huanjing Kexue* **2016**, *37*, 710–716.
31. Hou, S.N.; Zheng, N.; Tang, L.; Ji, X.F.; Li, Y.Y.; Hua, X.Y. Pollution characteristics, sources, and health risk assessment of human exposure to Cu, Zn, Cd and Pb pollution in urban street dust across China between 2009 and 2018. *Environ. Int.* **2019**, *128*, 430–437. [CrossRef] [PubMed]
32. He, Y.; Peng, C.; Zhang, Y.; Guo, Z.; Xiao, X.; Kong, L. Comparison of heavy metals in urban soil and dust in cities of China: Characteristics and health risks. *Int. J. Environ. Sci. Technol.* **2023**, *20*, 2247–2258. [CrossRef]
33. Kumar, M.; Furumai, H.; Kurisu, F.; Kasuga, I. Tracing source and distribution of heavy metals in road dust, soil and soakaway sediment through speciation and isotopic fingerprinting. *Geoderma* **2013**, *211*, 8–17. [CrossRef]
34. Chen, H.Y.; Teng, Y.G.; Lu, S.J.; Wang, Y.Y.; Wang, J.S. Contamination features and health risk of soil heavy metals in China. *Sci. Total Environ.* **2015**, *512*, 143–153. [CrossRef]
35. Briffa, J.; Sinagra, E.; Blundell, R. Heavy metal pollution in the environment and their toxicological effects on humans. *Heliyon* **2020**, *6*, e04691. [CrossRef]
36. Li, Y.; Ye, Z.; Yu, Y.; Li, Y.; Jiang, J.; Wang, L.J.; Wang, G.M.; Zhang, H.C.; Li, N.; Xie, X. A combined method for human health risk area identification of heavy metals in urban environments. *J. Hazard. Mater.* **2023**, *449*, 131067. [CrossRef]

37. Meena, M.; Meena, B.S.; Chandrawat, U.; Rani, A. Seasonal variation of selected metals in particulate matter at an industrial city Kota, India. *Aerosol Air Qual. Res.* **2016**, *16*, 990–999. [CrossRef]
38. Choi, E.; Yi, S.-M.; Lee, Y.S.; Jo, H.; Baek, S.-O.; Heo, J.-B. Sources of airborne particulate matter-bound metals and spatial-seasonal variability of health risk potentials in four large cities, South Korea. *Environ. Sci. Pollut. Res.* **2022**, *29*, 28359–28374. [CrossRef]
39. Feng, J.S.; Song, N.N.; Yu, Y.X.; Li, Y.X. Differential analysis of FA-NNC, PCA-MLR, and PMF methods applied in source apportionment of PAHs in street dust. *Environ. Monit. Assess.* **2020**, *192*, 727. [CrossRef]
40. Wang, X.Y.; Liu, E.F.; Yan, M.X.; Zheng, S.W.; Fan, Y.; Sun, Y.X.; Li, Z.J.; Xu, J.L. Contamination and source apportionment of metals in urban road dust (Jinan, China) integrating the enrichment factor, receptor models (FA-NNC and PMF), local Moran's index, Pb isotopes and source-oriented health risk. *Sci. Total Environ.* **2023**, *878*, 163211. [CrossRef]
41. Aryal, R.; Beecham, S.; Sarkar, B.; Chong, M.N.; Kinsela, A.; Kandasamy, J.; Vigneswaran, S. Readily wash-off road dust and associated heavy metals on motorways. *Water Air Soil Pollut.* **2017**, *228*, 1. [CrossRef]
42. Jeong, H.; Choi, J.Y.; Lee, J.; Lim, J.; Ra, K. Heavy metal pollution by road-deposited sediments and its contribution to total suspended solids in rainfall runoff from intensive industrial areas. *Environ. Pollut.* **2020**, *265*, 115028. [CrossRef] [PubMed]
43. Olken, F.; Rotem, D. Random sampling from databases: A survey. *Stat. Comput.* **1995**, *5*, 25–42. [CrossRef]
44. Muller, G. Index of geoaccumulation in sediments of the Rhine River. *GeoJournal* **1969**, *2*, 109–118.
45. Lu, X.W.; Li, L.Y.; Wang, L.J.; Lei, K.; Huang, J.; Zhai, Y.X. Contamination assessment of mercury and arsenic in roadway dust from Baoji, China. *Atmos. Environ.* **2009**, *43*, 2489–2496. [CrossRef]
46. Pathak, A.K.; Kumar, R.; Kumar, P.; Yadav, S. Sources apportionment and spatio-temporal changes in metal pollution in surface and sub-surface soils of a mixed type industrial area in India. *J. Geochem. Explor.* **2015**, *159*, 169–177. [CrossRef]
47. Cheng, H.X.; Li, K.; Li, M.; Yang, K.; Liu, F.; Cheng, X.M. Geochemical background and baseline value of chemical elements in urban soil in China. *Earth Sci. Front.* **2014**, *21*, 265–306.
48. Yang, Z.P.; Li, X.Y.; Wang, Y.; Chang, J.Z.; Liu, X.R. Trace element contamination in urban topsoil in China during 2000–2009 and 2010–2019: Pollution assessment and spatiotemporal analysis. *Sci. Total Environ.* **2021**, *758*, 143647. [CrossRef]
49. Zhang, X.X.; Zha, T.G.; Guo, X.P.; Meng, G.X.; Zhou, J.X. Spatial distribution of metal pollution of soils of Chinese provincial capital cities. *Sci. Total Environ.* **2018**, *643*, 1502–1513. [CrossRef]
50. Padoan, E.; Romè, C.; Ajmone-Marsan, F. Bioaccessibility and size distribution of metals in road dust and roadside soils along a peri-urban transect. *Sci. Total Environ.* **2017**, *601*, 89–98. [CrossRef]
51. Shi, D.Q.; Lu, X.W.; Wang, Q. Evaluating Health Hazards of Harmful Metals in Roadway Dust Particles Finer than 100 μm. *Pol. J. Environ. Stud.* **2018**, *27*, 2729–2737. [CrossRef] [PubMed]
52. *GB36600-2018*; Soil Environmental Quality—Risk Control Standard for Soil Contamination of Development Land. Chinese Standard: Beijing, China, 2018.
53. Oliver, M.A.; Webster, R. Kriging: A method of interpolation for geographical information systems. *Int. J. Geogr. Inf. Syst.* **1990**, *4*, 313–332. [CrossRef]
54. Largueche, F.-Z.B. Estimating soil contamination with Kriging interpolation method. *Am. J. Appl. Sci.* **2006**, *3*, 1894–1898. [CrossRef]
55. Sedgwick, P. Pearson's correlation coefficient. *BMJ* **2012**, *345*, e4483. [CrossRef]
56. Jin, Y.L.; O'Connor, D.; Ok, Y.S.; Tsang, D.C.; Liu, A.; Hou, D. Assessment of sources of heavy metals in soil and dust at children's playgrounds in Beijing using GIS and multivariate statistical analysis. *Environ. Int.* **2019**, *124*, 320–328. [CrossRef]
57. Abdi, H.; Williams, L.J. Principal component analysis. *Wiley Interdiscip. Rev. Comput. Stat.* **2010**, *2*, 433–459. [CrossRef]
58. Li, S.Y.; Zhang, Q.F. Risk assessment and seasonal variations of dissolved trace elements and heavy metals in the Upper Han River, China. *J. Hazard. Mater.* **2010**, *181*, 1051–1058. [CrossRef]
59. Shi, D.Q.; Lu, X.W. Accumulation degree and source apportionment of trace metals in smaller than 63 μm road dust from the areas with different land uses: A case study of Xi'an, China. *Sci. Total Environ.* **2018**, *636*, 1211–1218. [CrossRef]
60. Yuan, R.Y.; Zheng, T.Y.; Zheng, X.L.; Liu, D.S.; Xin, J.; Yu, L.; Liu, G.Q. Identification of groundwater nitrate pollution sources in agricultural area using PCA and SIAR methods. *Episodes* **2020**, *43*, 739–749. [CrossRef]
61. Yan, B.; Xu, D.M.; Chen, T.; Yan, Z.A.; Li, L.L.; Wang, M.H. Leachability characteristic of heavy metals and associated health risk study in typical copper mining-impacted sediments. *Chemosphere* **2020**, *239*, 124748. [CrossRef]
62. Aguilera, A.; Bautista, F.; Gutiérrez-Ruiz, M.; Ceniceros-Gómez, A.E.; Cejudo, R.; Goguitchaichvili, A. Heavy metal pollution of street dust in the largest city of Mexico, sources and health risk assessment. *Environ. Monit. Assess.* **2021**, *193*, 193. [CrossRef] [PubMed]
63. Wang, S.; Cai, L.M.; Wen, H.H.; Luo, J.; Wang, Q.S.; Liu, X. Spatial distribution and source apportionment of heavy metals in soil from a typical county-level city of Guangdong Province, China. *Sci. Total Environ.* **2019**, *655*, 92–101. [CrossRef] [PubMed]
64. Sun, L.; Guo, D.K.; Liu, K.; Meng, H.; Zheng, Y.J.; Yuan, F.Q.; Zhu, G.H. Levels, sources, and spatial distribution of heavy metals in soils from a typical coal industrial city of Tangshan, China. *Catena* **2019**, *175*, 101–109. [CrossRef]
65. Luo, H.P.; Wang, Q.Z.; Guan, Q.Y.; Ma, Y.R.; Ni, F.; Yang, E.Q.; Zhang, J. Heavy metal pollution levels, source apportionment and risk assessment in dust storms in key cities in Northwest China. *J. Hazard. Mater.* **2022**, *422*, 126878. [CrossRef] [PubMed]
66. Ma, X.; Sha, Z.P.; Li, Y.Z.; Si, R.T.; Tang, A.H.; Fangmeier, A.; Liu, X.J. Temporal-spatial characteristics and sources of heavy metals in bulk deposition across China. *Sci. Total Environ.* **2024**, *926*, 171903. [CrossRef]

67. Trujillo-González, J.M.; Torres-Mora, M.A.; Keesstra, S.; Brevik, E.C.; Jiménez-Ballesta, R. Heavy metal accumulation related to population density in road dust samples taken from urban sites under different land uses. *Sci. Total Environ.* **2016**, *553*, 636–642. [CrossRef]
68. Skrbic, B.D.; Buljovcic, M.; Jovanovic, G.; Antic, I. Seasonal, spatial variations and risk assessment of heavy elements in street dust from Novi Sad, Serbia. *Chemosphere* **2018**, *205*, 452–462. [CrossRef]
69. Liu, J.W.; Kang, H.; Tao, W.D.; Li, H.Y.; He, D.; Ma, L.X.; Tang, H.J.; Wu, S.Q.; Yang, K.X.; Li, X.X. A spatial distribution–Principal component analysis (SD-PCA) model to assess pollution of heavy metals in soil. *Sci. Total Environ.* **2023**, *859*, 160112. [CrossRef]
70. Pandey, B.; Agrawal, M.; Singh, S. Assessment of air pollution around coal mining area: Emphasizing on spatial distributions, seasonal variations and heavy metals, using cluster and principal component analysis. *Atmos. Pollut. Res.* **2014**, *5*, 79–86. [CrossRef]
71. Meuser, H.; Meuser, H. Causes of Soil Contamination in the Urban Environment. In *Contaminated Urban Soils*; Springer: Berlin/Heidelberg, Germany, 2010; pp. 29–94.
72. Li, G.; Sun, G.X.; Ren, Y.; Luo, X.S.; Zhu, Y.G. Urban soil and human health: A review. *Eur. J. Soil Sci.* **2018**, *69*, 196–215. [CrossRef]
73. Mukherjee, A.B.; Zevenhoven, R.; Brodersen, J.; Hylander, L.D.; Bhattacharya, P. Mercury in waste in the European Union: Sources, disposal methods and risks. *Resour. Conserv. Recycl.* **2004**, *42*, 155–182. [CrossRef]
74. Cheng, H.F.; Hu, Y.A. Mercury in municipal solid waste in China and its control: A review. *Environ. Sci. Technol.* **2012**, *46*, 593–605. [CrossRef] [PubMed]
75. Westerlund, C.; Viklander, M. Particles and associated metals in road runoff during snowmelt and rainfall. *Sci. Total Environ.* **2006**, *362*, 143–156. [CrossRef] [PubMed]
76. Huston, R.; Chan, Y.; Chapman, H.; Gardner, T.; Shaw, G. Source apportionment of heavy metals and ionic contaminants in rainwater tanks in a subtropical urban area in Australia. *Water Res.* **2012**, *46*, 1121–1132. [CrossRef]
77. Hussain, K.; Rahman, M.; Prakash, A.; Hoque, R.R. Street dust bound PAHs, carbon and heavy metals in Guwahati city–Seasonality, toxicity and sources. *Sustain. Cities Soc.* **2015**, *19*, 17–25. [CrossRef]
78. Han, L.H.; Zhuang, G.S.; Cheng, S.Y.; Wang, Y.; LI, J. Characteristics of re-suspended road dust and its impact on the atmospheric environment in Beijing. *Atmos. Environ.* **2007**, *41*, 7485–7499. [CrossRef]